Published in final edited form as:
J Bone Miner Res. 2013 June ; 28(6): 1422–1433. doi:10.1002/jbmr.1857.

Augmentation of Smad-dependent BMP signaling in neural crest cells causes craniosynostosis in mice

Yoshihiro Komatsu[1,2], **Paul B. Yu**[3], **Nobuhiro Kamiya**[1,2,4], **Haichun Pan**[1], **Tomokazu Fukuda**[2,5], **Gregory J. Scott**[6], **Manas K. Ray**[6], **Ken-ichi Yamamura**[7], and **Yuji Mishina**[1,2,6]

[1]Department of Biologic and Materials Sciences, School of Dentistry, University of Michigan, Ann Arbor, MI 48109, USA

[2]Laboratory of Reproductive and Developmental Toxicology, National Institute of Environmental Health Sciences, National Institutes of Health, Research Triangle Park, NC 27709, USA

[3]Division of Cardiology, Department of Medicine, Massachusetts General Hospital and Harvard Medical School, Thier 505, 50 Blossom Street, Boston, MA 02114, USA

[4]Center for Excellence in Hip Disorders, Texas Scottish Rite Hospital for Children, Dallas, TX 75219, USA

[5]Graduate School of Agricultural Science, Tohoku University, Sendai 981-8555, Japan

[6]Knock Out Core, National Institute of Environmental Health Sciences, National Institutes of Health, Research Triangle Park, NC 27709, USA

[7]Institute of Molecular Embryology and Genetics, Kumamoto University, Kumamoto 860-0811, Japan

Abstract

Craniosynostosis describes conditions in which one or more sutures of the infant skull are prematurely fused, resulting in facial deformity and delayed brain development. Approximately 20% of human craniosynostoses are thought to result from gene mutations altering growth factor signaling; however, the molecular mechanisms by which these mutations cause craniosynostosis are incompletely characterized, and the causative genes for diverse types of syndromic craniosynostosis have yet to be identified. Here, we show that enhanced bone morphogenetic protein (BMP) signaling through the BMP type IA receptor (BMPR1A) in cranial neural crest cells, but not in osteoblasts, causes premature suture fusion in mice. In support of a requirement for precisely regulated BMP signaling, this defect was rescued on a *Bmpr1a* haploinsufficient background, with corresponding normalization of Smad phosphorylation. Moreover, in vivo treatment with LDN-193189, a selective chemical inhibitor of BMP type I receptor kinases resulted in partial rescue of craniosynostosis. Enhanced signaling of the fibroblast growth factor (FGF) pathway, which has been implicated in craniosynostosis, was observed in both mutant and rescued mice, suggesting that augmentation of FGF signaling is not the sole cause of premature fusion found in this model. The finding that relatively modest augmentation of Smad-dependent BMP signaling leads to premature cranial suture fusion suggests an important contribution of dysregulated BMP signaling to syndromic craniosynostoses, and potential strategies for early intervention.

Corresponding author: Yuji Mishina, Ph.D. Department of Biologic and Materials Sciences School of Dentistry, University of Michigan 1011 N. University Ave., Ann Arbor, MI 48109, USA. Tel: +1-734-763-5579, Fax: +1-734-647-2110, mishina@umich.edu.

Keywords

BMP; Craniosynostosis; Neural crest cells; Smad-signaling; Suture

Introduction

Craniosynostosis, a syndrome of premature fusion of cranial sutures, affects one in 2,500 live births (1,2). This condition results in facial deformity and restricted brain growth, with challenging clinical management that often requires multiple corrective surgeries. Individuals with craniosynostosis left untreated during infancy develop increased intracranial pressure that can cause chronic headaches and gradual loss of vision, and are at risk for cognitive impairment. Craniofacial abnormalities seen with craniosynostosis can also cause upper airway obstruction and sleep apnea (3).

Craniosynostosis is a devastating disorder, for which the only treatment is carefully timed and extensive reconstructive surgery. Although advances in molecular genetics past decades have revealed several gene mutations which can result in craniosynostosis, the molecular pathophysiology of craniosynostosis in humans remains incompletely understood. Limited cases of syndromic craniosynostoses (20-30%) have been found to be associated with the mutations of fibroblast growth factor receptor family (FGFR1, FGFR2 and FGFR3), MSX2, TWIST1 and EFNB1 in man; however, the genetic basis of most craniosynostoses have yet to be identified (1,2). Craniosynostosis has diverse presentations, which include the Apert, Boston, Crouzon, Pfeiffer, Jackson-Weiss and Saethre-Chotzen syndromes (1,2). While coronal sutures are commonly affected in these syndromes, each syndrome has a unique pattern of suture fusions. For example, the sagittal suture is frequently fused in both Crouzon and Pfeiffer syndromes but not in Saethre-Chotzen syndrome. The unique pattern of fusion in each syndrome suggests that distinct developmental processes underlie various premature suture fusion phenotypes. Defining the molecular and cellular pathogenesis of each syndromic craniosynostosis could facilitate strategies for the early identification, prevention or treatment of these developmental defects.

Bone morphogenetic proteins (BMPs) play broad roles in developmental patterning, including skull morphogenesis (4-7). Gain-of-function mutations in MSX2, a member of the homeobox gene family whose transcription is regulated by BMP and TGF-β signaling, result in an autosomal dominant Boston-type craniosynostosis in man, while mice overexpressing *Msx2* also develop premature fusion of coronal and sagittal sutures (8,9). Moreover, the endogenous BMP antagonist noggin is expressed in non-fusing sutures, and is observed to enforce suture patency in mice (10). These prior observations suggest that appropriate levels of BMP signaling may be critical for maintaining normal suture patency during skull development and that dysregulated BMP signaling may contribute to craniosynostosis.

Since the frontal region of cranial bones and sutures are derived from a distinct multipotent cell population, i.e., cranial neural crest (CNC) cells (11-13), we hypothesized that aberrant differentiation of CNC cells caused by alterations in BMP signaling results in cranial malformations. To test this hypothesis, we developed a conditional mouse model with enhanced BMP signaling in the skull and sutures. We found that failure to maintain precisely controlled Smad-dependent BMP signaling in CNC cells but not in osteoblast-committed cells led to craniosynostosis. We also found that reduction of BMP signaling by genetic or pharmacological methods rescued the premature fusion found in the metopic suture, as well as abnormalities found in CNC-derived skull bones. In this enhanced BMP signaling model, we also observed enhanced FGF ligand expression. However, these perturbations in FGF signaling did not appear to account for craniosynostosis, in contrast to

the phenotypes observed in FGF gain-of-function mutant mice (14-17). These results lend novel mechanistic support for the concept that supraphysiological levels of BMP signaling contribute to some human craniosynostoses, which in turn might be mitigated by pharmacologic blockade early in their genesis.

Materials and Methods

Generation of ca-Bmpr1a mouse lines

A plasmid containing human *BMPR1A* cDNA with a Q233D mutation was kindly obtained from Dr. T. Imamura (Cancer Institute of Japan). The cDNA fragment was inserted into a *Pst*I site of the CAG-Z-EGFP vector (18,19). The transgenic vector was linearized and electroporated into AB2.2 mouse ES cells (Lexicon Genetics) with a PGKneobpA plasmid for selection with G418. Ninety-six G418 resistant colonies were stained for β-gal activity to confirm the expression of the transgene. Four of representative ES clones, which showed relatively strong expressions of β-gal activity, were injected into blastocysts from C57BL/6 mice, and 3 of them (clones A3, F1 and F2) underwent germline transmission. Progenies bred with wild-type C57BL/6 showed expected ration of transmission of the transgene (50%), indicating that transgenic mouse lines have a single integration site for transgene in its genome. We initially analyzed progenies from clone A3 and F1 to confirm that they developed identical phenotypes (Fig. S1), thus we focused transgenic line from clone A3 in the rest of analyses. *P0-Cre* mouse, C57BL/6J-Tg(P0-Cre)94Imeg (ID 148), was provided by CARD, Kumamoto University, Japan. All mouse experiments were performed in accordance with National Institute of Environmental Health Sciences and University of Michigan guidelines covering the humane care and use of animals in research.

Histology, skeletal staining, immunohistochemistry and micro-CT (μCT)

Embryos were fixed in either 10% formalin or 4% paraformaldehyde, embedded in paraffin, and stained with Hematoxylin and Eosin (H&E). Cranial bone was stained with alizarin red and alcian blue by standard methods. For immunohistochemistry, mouse skull was fixed with 4% paraformaldehyde at 4°C overnight and replaced with 20% sucrose in PBS at 4°C. Samples were embedded by O.C.T. compound and 10μm cryo-sections were cut. After washing with PBS containing 0.1% Triton X-100, the specimens were incubated with rabbit anti-FGF2 (dilution 1:100, catalog number: AB1458, Chemicon), rabbit anti-FGFR1 (dilution 1:100, catalog number: sc-121, Santa Cruz), rabbit anti-FGFR2 (dilution 1:100, catalog number: sc-122, Santa Cruz), rabbit anti-phospho-p38 MAPK (dilution 1:50, catalog number: 4631, Cell Signaling) and rabbit anti-phospho-SMAD1/5/8 (dilution 1:100, catalog number: 9511, Cell Signaling) at 4°C overnight, with Alexa Fluor 488 donkey anti-rabbit IgG (dilution 1:100, catalog number: A21206, Invitrogen) used as secondary Ab. Sections were mounted with ProLong Gold antifade reagent with DAPI (catalog number: P36935, Invitrogen). Fluorescence images were obtained with an Olympus BX-51 microscope with an Olympus DP-70 CCD camera. Captured images were processed in Adobe Photoshop CS3 (version 10.0). Skulls were scanned using a micro-computed tomography (μCT) system at 12mm of thickness, 55kV of energy and 145mA of intensity (μCT40: Scanco Medical AG, Brüttisellen Switzerland), and reconstructed to produce 2D and 3D images (20).

Quantitative real time RT-PCR

Skull tissues were pretreated with RNA later (Ambion) and RNA isolated using TRIzol (Invitrogen). cDNA was synthesized by using SuperScript III cDNA Synthesis (Invitrogen). TaqMan probes were purchased and real time RT-PCR was performed by ABI PRISM 7500 (Applied Biosystems). Data were normalized to GAPDH by $2^{-\Delta\Delta Ct}$ method.

Establishment of preosteoblast cells from the skull

Cranial preosteoblasts were established from newborn pups as described previously (13,21). Preosteoblasts were grown in Minimum Essential Medium (alpha-MEM) (catalog number: 12561, Invitrogen) with 10% fetal bovine serum (Hyclone) and penicillin/streptomycin (catalog number: P-0781, Sigma). 100μg/ml ascorbic acid (catalog number: A-4403, Sigma) and 4mM β-glycerophosphate (catalog number: G-9891, Sigma) were added for further primary cultures.

Cell culture and immunoblot analysis

Preosteoblasts were stimulated with recombinant human BMP2 (catalog number: 355-BM, R&D) or FGF1 (catalog number: 232-FA, R&D) depended on each experimental time course. RIPA buffer (20mM Tris-HCl, 0.1% SDS, 1% Triton X-100, 1% sodium deoxycholate) was used for preparation of cell extracts. Subsequently, cell lysates were separated by SDS-PAGE and transferred to Amersham Hybond-P membrane (GE Healthcare). Immunoblotting was performed with rabbit anti-phospho-SMAD1/5/8 (9511), rabbit anti-phospho-p44/42 MAPK (ERK1/2) (4376), rabbit anti-p44/42 MAP Kinase (4695), rabbit anti-phospho-p38 MAPK (4631), rabbit anti-p38 MAP Kinase (9212), rabbit anti-phospho-SAPK/JNK (4668), rabbit anti-SAPK/JNK (9258), rabbit anti-phospho-TAK1 (9399) and rabbit anti-TAK1 (4505), all from Cell Signaling. Mouse anti-β actin (catalog number: A-5441, Sigma) and rabbit anti-GAPDH (catalog number: 2118, Cell Signaling) were used as a loading control. Signal detection was performed by ECL western blotting detection reagents (GE Healthcare).

Treatment of animals with aqueous LDN-193189

LDN-193189 was dissolved in sterile endotoxin-free water (22). A dose of 2.5 mg of the LDN-193189 per kg body weight per day was injected intraperitoneally into pregnant mice on days E14 through E18 and continued through P15 to nursing dams.

Results

Generation of constitutively active form of Bmpr1a mice and validation of neural crest-specific Cre mice

To target enhanced BMP signaling to the cranial neural crest (CNC) cells, we generated transgenic mice that conditionally express a constitutively active form of *Bmpr1a* (*ca-Bmpr1a*) (Fig. S2A). A mutation of Gln residue 233 to Asp (Q233D) of the glycineserine (GS) rich kinase regulatory domain of *Bmpr1a* is known to result in constitutive activation of the type I receptor kinase activity (23). We bred these mice with *P0-Cre* mice, which express a Cre-recombinase transgene under control of a neural crest-specific promoter (24). This genetic manipulation enhances BMP signaling specifically in neural crest-derived tissues. We confirmed localization of *P0-Cre* expressing cells in the skull using ROSA26 reporter line (25) (Fig. S2). LacZ positive cells were observed in nasal-frontal bones and the metopic suture as expected (11), consistent with efficient targeting of CNC-derived cells by the *P0-Cre* transgene during skull development.

Enhanced BMP signaling through ca-BMPR1A in cranial neural crest cells causes craniosynostosis

The mutant mice, which carried both *ca-Bmpr1a* and *P0-Cre* transgenes (*ca-Bmpr1a:P0-Cre*, or mutant (MT), hereafter), showed enhanced levels of SMAD1/5/8 phosphorylation without ligand stimulation in CNC derived-preosteoblast cells from skull that were further increased by BMP2 ligand treatment (Fig. S2B). These mutant mice displayed short broad snouts and orbital hypertelorism (Fig. 1A-D). Skeletal staining at postnatal day 17 (P17) and

histological observation at P8 revealed premature fusion of the anterior frontal (AF) suture in *ca-Bmpr1a:P0-Cre*, while AF sutures in control mice retained patency (Fig. 1E-H). Other sutures including the coronal suture developed normally (Fig. S4), and no bones were missing in skull base of mutant mice (Fig. S5). Calvaria from *ca-Bmpr1a:P0-Cre* were thinner (Fig. 1G, H), resembling a phenotype found in a mouse model of Apert syndrome harboring a mutation in *Fgfr2* (Ser252Trp) representing one of the most severe forms of craniosynostosis. Interestingly, we found evidence of increased apoptosis in mutant mice at newborn stage (Fig. S6), consistent with the thin calvaria found in *ca-Bmpr1a:P0-Cre* (Fig. 1G, H) and in certain syndromes such as Apert type craniosynostosis (21,26-30).

Since our mutant mice showed increased levels of Smad signaling in neural crest-derived tissues including osteoblasts, one of the immediate hypotheses to be examined is that the enhanced BMP signaling in differentiated osteoblasts stimulates their proliferation and/or differentiation to ossify suture mesenchyme. Thus, first we investigated the proliferative and differentiation capability of the mutant osteoblasts. However, there were no significant differences in the ability of skull-derived preosteoblasts to proliferate or differentiate (Fig. S7). Next, we bred *ca-Bmpr1a* mice with *Col1-CreER™* (*ca-Bmpr1a:Col1-CreER™*) (31) to activate BMP signaling in an osteoblast-specific manner to examine if enhanced BMP signaling through BMPR1A exerts its effects through osteoblast-lineage committed cells during skull development. While *Col1-CreER™* showed the robust Cre recombination in whole skull in our previous study (31), *ca-Bmpr1a:Col1-CreER™* mice did not display any of the skull abnormalities seen in *ca-Bmpr1a:P0-Cre* mice (Fig. S8). Such striking phenotypic differences between neural crest-specific and osteoblast-specific activation of BMP signaling reveal the critical role of BMP signaling in neural crest-derived multipotent cells rather in the osteoblast-committed lineages for governing normal skull development by regulating suture patency.

FGF components and FGF signaling are upregulated in enhanced BMP signaling mutants

Because upregulated FGF signaling results in craniosynostosis (15,16,32-34), as exemplified by Apert syndrome (14,17,35), we speculated that enhanced BMP signaling through BMPR1A might positively regulate FGF signaling or components of its pathway leading to premature suture fusion. We first analyzed the expression of FGF pathway components in the skull by immunohistochemistry at embryonic day (E) 17.5. In the AF sutures of mutant embryos, levels of FGF2, FGFR1 and FGFR2 were significantly upregulated (Fig. 2A). Consistent with the upregulation of FGF ligand and receptors in mutant embryos, phosphorylated ERK1/2 (*p*-ERK1/2), a known effector of FGF signaling, was dramatically increased in mutant skull bones and metopic sutures (Fig. 2B). Using preosteoblasts established from CNC-derived skull bones (nasal and frontal), we observed that higher levels of *p*-ERK1/2 were induced with BMP2 stimulation in mutant preosteoblasts compared with control preosteoblasts (Fig. 2C, D). Taken together, these results suggest that enhanced BMP signaling through BMPR1A in CNC cells might upregulate or synergize with FGF signaling to promote craniosynostosis, which we examined further as below.

Augmentation of FGF signaling is not the direct cause to develop skull malformation in enhanced BMP signaling mutants

To help confirm that the *ca-Bmpr1a* transgene exerted its effects on both skull and suture abnormalities via excess BMP signaling, we tested the impact of decreased wild-type *Bmpr1a* gene dosage by superimposing *Bmpr1a* heterozygosity (*Bmpr1a*$^{+/-}$) (36) on the *ca-Bmpr1a:P0-Cre* double transgenic background. Notably, *ca-Bmpr1a:P0-Cre* carrying one copy of endogenous *Bmpr1a* (*ca-Bmpr1a:P0-Cre:Bmpr1a*$^{+/-}$, rescued; R, n=7) showed normal head morphology that was comparable with controls (control; CT, n=7), whereas *ca-Bmpr1a:P0-Cre* littermates with two copies of endogenous *Bmpr1a* retained the

craniosynostosis phenotype (mutant; MT, n=7) (Fig. 3A). We confirmed the patency of AF sutures in rescued mice by skeletal staining and histological analysis (Fig. 3A). We also noted that skull bone thickness in rescued mice was comparable to that of control mice (Fig. 3A). We further examined the expression level of *Bmpr1a* among control, *ca-Bmpr1a:P0-Cre* and *ca-Bmpr1a:P0-Cre:Bmpr1a*$^{+/-}$ preosteoblast cells by quantitative real time RT-PCR (qRT-PCR). *Bmpr1a* expression was reduced by more than half in *ca-Bmpr1a:P0-Cre:Bmpr1a*$^{+/-}$ cells as compared with both control and *ca-Bmpr1a:P0-Cre* preosteoblast cells (Fig. 3B). Expression levels of the transgene were very low when assessed using transgene-specific primers by qRT-PCR (data not shown), explaining the observation that levels of *Bmpr1a* expression in the mutants (when measuring transcripts both from the endogenous locus and the transgene) were comparable with those in controls. These results demonstrate that the increase in BMP signaling mediated by *ca-Bmpr1a* transgene is relatively modest in that the loss of one wild-type allele may compensate, and consequently that precise regulation of BMP signaling is critical for maintaining suture patency and normal skull morphogenesis.

Since FGF signaling was also upregulated in mutant skulls (Fig. 2), we speculated that increased BMP signaling in CNC cells might enhance FGF signaling to cause premature suture fusion in *ca-Bmpr1a:P0-Cre* mice. To compare the regulation of FGF signaling molecules in normal and mutant skulls, we examined their levels of expression in nasal-frontal bones by qRT-PCR. On one hand, the expression of *Fgf2*, *Fgfr1*, *Fgfr2,* components for the FGF signaling, and *Sprouty1/2/3/4*, downstream targets for the FGF signaling, in mutant (MT) mice were enhanced compared with control (CT) mice (Fig. 3C), suggesting enhanced FGF signaling accompanies enhanced BMP signaling in this model. However, the expression of these genes was comparable between mutant (MT) and rescued (R) mice (Fig. 3C). Furthermore, we found comparable levels of *p*-ERK1/2 in mutant (MT) and rescued (R) preosteoblasts, which still showed a higher degree of ERK1/2 activation as compared with control (CT) preosteoblasts (Fig. 3D). These results suggest that the rescue of the craniosynostosis phenotype in compound inducible-transgenic and haploinsufficient mice was not due to the normalization of FGF-ERK1/2 signaling.

Enhanced Smad-dependent BMP signaling pathway is responsible for the etiology of craniosynostosis

Upregulated FGF/ERK signaling did not appear to account for skull development abnormalities observed in *ca-Bmpr1a:P0-Cre* mice (Fig. 3C, D). We investigated other potential explanations of how enhanced Smad-dependent or -independent BMP signaling might induce premature suture fusion in mutants via downstream intracellular signaling. We assessed activation of other mitogen-activated protein kinase (MAPK) pathways including p38, which are thought to be effectors of Smad-independent signaling by BMP and TGF-β ligands (37). Consistent with findings of enhanced Smad activation in skull-derived preosteoblasts (Fig. S2B), mutant calvarium exhibited higher levels of phosphorylated SMAD1/5/8 (*p*-SMAD1/5/8) compared with controls (Fig. 4A). On the other hand, levels of phosphorylated p38 (*p*-p38) remained undetectable in both control and mutant skulls (Fig. 4A). In addition, BMP2 stimulation did not activate p38 or JNK beyond basal levels in skull-derived preosteoblasts (Fig. 4B). Moreover, levels of phosphorylated TGF-β-activated kinase 1 (TAK1), the MAPKKK functioning upstream of p38 and JNK (38), was comparable between control, mutant, and rescued preosteoblast cells (Fig. S9). The lack of modulation of TAK1 or specific MAPK pathways in mutant mouse tissues suggested that canonical Smad-dependent BMP signaling may be primarily responsible for the craniosynostosis phenotype. To investigate further the relationship between enhanced Smad-dependent BMP signaling and skull defects in *ca-Bmpr1a:P0-Cre*, we examined the kinetics of *p*-SMAD1/5/8 signaling in control, mutant and rescued preosteoblasts. As seen in the

mutant calvarium showing enhanced SMAD1/5/8 phosphorylation (Fig. 4A), mutant preosteoblasts (MT) displayed the higher basal levels of *p*-SMAD1/5/8 (at 0 min) and greater levels of *p*-SMAD1/5/8 in response to BMP2, which were restored in rescued presosteoblasts (R) to levels comparable to wild-type preosteoblasts (CT) (Fig. 4C, D). These findings strongly suggest that enhanced Smad-dependent BMP signaling is the principle etiology of craniosynostosis in *ca-Bmpr1a:P0-Cre* mice.

Treatment of selective chemical inhibitor of BMP type I receptor kinases partially rescues craniosynostosis phenotype in vivo

To assess further the role of enhanced Smad-dependent BMP signaling in the skull malformation phenotype, we used a selective chemical inhibitor for BMP type I receptor kinases, LDN-193189 (22,39) as a means for normalizing Smad-dependent signaling. Since LDN-193189 and other chemical kinase inhibitors are known to possess various off-target effects (40), we validated the selectivity of LDN-193189 for Smad-dependent BMP signaling in our tissues. We measured levels of *p*-SMAD1/5/8 with varying concentrations of LDN-193189 using wild-type preosteoblasts from neural crest-derived bones in skull. Similar to what was previously reported (22), in skull-derived preosteoblasts low concentrations of LDN-193189 (~50 nM) were sufficient to inhibit BMP mediated phosphorylation of SMAD1/5/8 without affecting Smad-independent signaling pathways (Fig. 5A, left panel). We further examined the potential impact of LDN-193189 upon levels of *p*-TAK1, *p*-ERK1/2 and *p*-p38 induced by FGF stimulation (Fig. 5A, right panel), confirming the activity of LDN-193189 as a selective inhibitor of Smad-mediated BMP signaling in CNC-derived preosteoblasts. We next explored the efficacy of LDN-193189 in the pre-natal prophylaxis of craniosynostosis in *ca-Bmpr1a:P0-Cre*. LDN-193189 was administered (2.5 mg/kg per day i.p.) to pregnant *ca-Bmpr1a* females after timed mating with *P0-Cre* males starting at E14.5 (Fig. 5B). After birth, lactating dams continued to receive LDN-193189 through P15, and neonates were euthanized at P16. Importantly, the cranial morphology of *ca-Bmpr1a:P0-Cre* treated in utero and perinatally with LDN-193189 was normalized (Fig. 5C). The length of nasal bones (n=5/6) and the shape of foramina in frontal bones (n=3/6) were normalized to that of control mice. Interestingly, prenatal LDN-193189 treatment did not visibly affect normal skull development in control pups (n=6/6) (Fig. 5C). Bone volume and trabecular number were decreased and trabecular spaces were wider in nasal and frontal bones of *ca-Bmpr1a:P0-Cre*, but were also normalized after LDN-193189 treatment (Fig. 5D). These results demonstrate that prenatal and perinatal treatment with a selective chemical inhibitor of BMP type I receptor kinases can partially rescue craniosynostosis in vivo, further supporting the importance of precisely regulated Smad-signaling in this phenotype.

Discussion

Our genetic study demonstrates that tightly controlled levels of Smad-dependent BMP signaling through BMPR1A in cranial neural crest (CNC) cells, not in committed osteoblasts, are critical for regulating suture patency and normal skull morphogenesis, whereas excessive signaling leads to craniosynostosis. Underneath molecular mechanisms of our findings are summarized in Fig. 6. In wild-type, BMPR1A exerts both Smad-dependent and -independent signaling upon BMP ligand binding. In the mutant mice (*ca-Bmpr1a:P0-Cre*), the basal levels of Smad-dependent signaling are upregulated and further increased upon BMP ligand binding. Increases of *p*-ERK1/2 are also observed, not due to the increase of Smad-independent signaling mediated by TAK1, but due to the increase of FGF signaling (Fig. S9). In the rescued mice (*ca-Bmpr1a:P0-Cre:Bmpr1a*$^{+/-}$), removal of one copy of endogenous *Bmpr1a* normalizes levels of Smad-dependent signaling leading to the phenotypic rescue of suture patency and skull morphology. Enhanced levels of FGF-ERK

signaling are still observed in the rescued mice. There are two outstanding questions why Smad-signaling enhanced by the constitutively activated BMPR1A is normalized by removal of one copy of the endogenous gene and why FGF signaling is still augmented in the rescued samples (see below for potential explanations). Although additional studies are necessary to answer these questions, our current results clearly demonstrate that a modest increase of BMP signaling via Smad-dependent signaling in CNC cells can be a cause of a premature suture fusion in our mouse model.

There is overwhelming evidence both in humans and mice that enhanced FGF signaling contributes to several types of craniosynostosis (1,2,41,42). Our mutant mice also exhibit upregulated FGF signaling; however, our model appears to be unique in that the enhanced levels of FGF signaling observed do not appear to be sufficient for the phenotype. Rather, the independent contribution of Smad-dependent BMP signaling in our model suggests an important and novel signaling mechanism for the etiology of craniosynostosis. Because associated gene mutations are identified in only 20-30% of human craniosynostosis (1,2) and each case shows diverse phenotypes such as positions of premature fusions and thickness of calvaria (26,35), some of the human cases may be developed by mutations in other signaling cascade than FGF signaling. Our findings suggest one of the possibilities that some of the human craniosynostosis are caused by misregulation of BMP signaling.

Since enhanced production of FGF ligands and receptors, and consequent activation of ERK1/2 are the causes of Apert syndrome (15-17,34), it is surprising that our compound transgenic/haploinsufficient mice exhibited upregulated FGF signaling in the face of essentially complete phenotypic rescue (Fig. 3B, C). One explanation may be that enhanced FGF signaling in *ca-Bmpr1a:P0-Cre* mice is not sufficient to induce morphological malformations, i.e., FGF signaling in *ca-Bmpr1a:P0-Cre* does not attain levels needed to develop craniosynostosis, as seen in $Fgfr2^{+/S252W}$ mice, for example (17). However, it is possible that the enhanced FGF signaling activity found in *ca-Bmpr1a:P0-Cre* mice may enhance pathogenesis of skull deformity, but only in the context of sufficient BMP signaling. While the mechanism of how enhanced BMP signaling upregulates the expression of FGF ligand, receptors and downstream components in mutant skulls is unclear, it has been reported that FGF receptor genes have Sp1 and Ap1 binding sequences in their promoters (43,44). Deletion of the Ap1 promoter sequence from a TGF-β and BMP-inducible gene disrupts BMP and TGF-β responsiveness (45), suggesting BMP signaling might regulate FGF via the Sp1/Ap1 promoter sequences. Thus, one could postulate that enhanced Smad-dependent BMP signaling may induce Sp1/Ap1 family transcriptional regulators that will bind to promoters of FGF receptors to enhance their expression in *ca-Bmpr1a:P0-Cre* mice. Subsequently, phospho-ERK1/2 may be evoked through the augmentation of FGF signaling in *ca-Bmpr1a:P0-Cre* mice. Further studies investigating the overlay of genetic or pharmacologic suppression of FGF signaling in our model would help to resolve this possibility.

The simplistic notion that excessive FGF-mediated signaling and cell growth drives the pathophysiology of craniosynostosis is complicated by the fact that craniosynostoses with enhanced FGF signaling are not always marked by enhanced proliferation and differentiation. Specifically, the FGFR2 C342Y mutation (Crouzon type craniosynostosis) inhibits preosteoblast differentiation and increases apoptosis in vitro (21). Moreover, Deng et al. found that the FGFR2 S252W mutation results in Apert type craniosynostosis in mice but did not observe changes in cell differentiation and proliferation, concluding that dysregulated apoptosis is involved in the pathogenesis of Apert type skull defects (26), consistent with our observations (Fig. S5). These observations and the present study support the concept that clinical phenotypes of craniosynostosis are quite divergent and cannot be accounted for by a single mechanism.

Craniosynostosis in *ca-Bmpr1a:P0-Cre* could be rescued by the loss of a single endogenous *Bmpr1a* allele (Fig. 3) suggests that a relatively small increment in levels of Smad-signaling results in the mutant phenotype, despite the use of an overexpressed and constitutively-active *Bmpr1a* transgene. Expression levels of *ca-Bmpr1a* transgene were quite low when assessed by qRT-PCR (data not shown), which may lead to the very modest increase of signaling associated with transgene. The completeness of rescue by heterozygosity, and the mildly enhanced ligand-independent and ligand-dependent BMP signaling observed in the tissues of these mice, and with other constitutively-active BMP type I receptor transgenes (22,46) suggest that the levels of BMP signaling attained by these strategies are only mildly supraphysiologic. The results from our pharmacological rescue also support this notion because the dose of LDN-193198 that did not influence skull morphology in the controls was capable to rescue the craniosynostotic phenotypes in the mutants (Fig. 5). Substantially larger increases in BMP signaling, especially during embryogenesis, lead to devastating outcomes (18,47). In contrast, constitutively-activating GS domain mutations of the BMP type I receptor *ACVR1* found in fibrodysplasia ossificans progressiva (48) permit survival to term with only mild morphological abnormalities, likely as a result of mildly increased activity of mutant protein expressed under endogenous promoter control (49). We interpret these data to suggest that moderate increases BMP signaling, for example caused by mutations in enhancer regions, could lead to craniosynostosis in the appropriate context, a possibility that has yet to be investigated in human studies. One interesting issue that remains to be addressed is whether the phenotypic rescue by heterozygosity of *Bmpr1a* is due to cell autonomous or non-cell autonomous effects. Using *Wnt1-Cre*, it was reported that nearly all cells in nasal and frontal bones are derived from CNC cells during skull development (2,11,13). Similarly, as shown in Fig.S3, we confirmed that *P0-Cre*, which we used in our study, could efficiently and specifically target to the CNC-derived cells in skull. We expect that in *ca-Bmpr1a:P0-Cre:Bmpr1a*$^{+/-}$ mice, virtually all cells in nasal and frontal bones in addition to the metopic suture possess a constitutively active *Bmpr1a* transgene along with loss of one allele of *Bmpr1a*. Thus, we are speculating that the skull abnormalities were rescued in a cell autonomous manner.

Both Smad-dependent and -independent BMP signaling pathways orchestrate cell fate, proliferation and differentiation in many tissues. Previous studies show that BMP signaling is critical for skull development (5,6,10,50-52). However, molecular mechanisms by which Smad-dependent and/or -independent BMP signaling regulate cranial development remain unknown. Regarding Smad-independent BMP signaling pathway, X-chromosome-linked inhibitor of apoptosis protein (XIAP) bridges BMPR1A and TAK1 and induces the activation of MAPK including p38 (53,54). One might hypothesize that augmentation of BMP signaling via ca-BMPR1A modulates TAK1 activity, which subsequently activates MAPK signaling pathway to cause craniosynostosis. However, we did not observe significant activation of TAK1 or MAPK p38 in mutant preosteoblasts (Fig. S9). The absence of modulation of TAK1 strongly argues against a role of MAPKs including p38 and JNK in our model; however, we cannot fully exclude the participation of other Smad-independent pathways contributing to the *Bmpr1a:P0-Cre* phenotype.

It has been known that FGFR tyrosine kinase inhibitors including PD173074 and PLX052 significantly prevent the premature suture fusion in organ culture level (16,55), and ERK/MAPK specific blocker U0126 successfully inhibits craniosynostosis in *Fgfr2*$^{+/S252W}$ mice (17). However, there are no known therapeutic interventions for other mechanisms of craniosynostosis. Since craniosynostoses have very diverse phenotypes (and likely mechanisms), successful strategies would identify chemopreventive reagents that target the specific etiology of each type of craniosynostosis. Our study employing a selective chemical inhibitor of BMP type I receptor kinases suggests a potential therapeutic strategy for prophylaxis of craniosynostosis caused by enhanced BMP signaling. Although it has not yet

been reported whether mutation(s) of *BMPRIA* cause craniosynostosis in human, our results suggest that treatment of LDN-193189 might be useful in craniosynostosis that is either caused by or facilitated by gain-of-function in BMP signaling. Identification of mutations or biomarkers signifying enhanced BMP signaling in CNC-derived tissues corresponding with syndromic or non-syndromic craniosynostosis would permit novel strategies for early identification and intervention for this challenging and incompletely characterized set of conditions.

Supplementary Material

Refer to Web version on PubMed Central for supplementary material.

Acknowledgments

We thank Dr. Wei Hsu for his generous teaching of calvarial preosteoblast culture techniques; Dr. Philippe Soriano for providing ROSA26 reporter mice; Ms. Toni Ward and Ms. Kelly McCann for maintaining mouse colonies; Drs. Mitsuo Yamauchi and Masaru Kaku for helping alkaline phosphatase analysis; Dr. Noriko Nakamura for helping western analysis; Ms. Michelle Lynch for helping micro-CT analysis; Drs. Sean Edwards, Toru Imamura and Jun Ninomiya-Tsuji for valuable suggestions; Drs. Paul Krebsbach and Rita Shiang for critical reading of this manuscript. This study is supported by the National Institutes of Health (K99DE021054 to Y.K., K08HL079943 and R01AR057374 to P.B.Y., R01DE020843 and ES071003-11 to Y.M.), a fellowship from the Japan Society for the Promotion of Science (Y.K.).

References

1. Wilkie AO, Morriss-Kay GM. Genetics of craniofacial development and malformation. Nat Rev Genet. 2001; 2(6):458–68. [PubMed: 11389462]
2. Morriss-Kay GM, Wilkie AO. Growth of the normal skull vault and its alteration in craniosynostosis: insights from human genetics and experimental studies. J Anat. 2005; 207(5):637–53. [PubMed: 16313397]
3. Renier D, Sainte-Rose C, Marchac D, Hirsch JF. Intracranial pressure in craniostenosis. J Neurosurg. 1982; 57(3):370–7. [PubMed: 7097333]
4. Urist MR. Bone: formation by autoinduction. Science. 1965; 150(698):893–9. [PubMed: 5319761]
5. Kim HJ, Rice DP, Kettunen PJ, Thesleff I. FGF-, BMP- and Shh-mediated signalling pathways in the regulation of cranial suture morphogenesis and calvarial bone development. Development. 1998; 125(7):1241–51. [PubMed: 9477322]
6. Ishii M, Han J, Yen HY, Sucov HM, Chai Y, Maxson RE Jr. Combined deficiencies of Msx1 and Msx2 cause impaired patterning and survival of the cranial neural crest. Development. 2005; 132(22):4937–50. [PubMed: 16221730]
7. Liu B, Yu HM, Hsu W. Craniosynostosis caused by Axin2 deficiency is mediated through distinct functions of beta-catenin in proliferation and differentiation. Dev Biol. 2007; 301(1):298–308. [PubMed: 17113065]
8. Liu YH, Kundu R, Wu L, Luo W, Ignelzi MA Jr. Snead ML, Maxson RE Jr. Premature suture closure and ectopic cranial bone in mice expressing Msx2 transgenes in the developing skull. Proc Natl Acad Sci U S A. 1995; 92(13):6137–41. [PubMed: 7597092]
9. Jabs EW, Muller U, Li X, Ma L, Luo W, Haworth IS, Klisak I, Sparkes R, Warman ML, Mulliken JB, et al. A mutation in the homeodomain of the human MSX2 gene in a family affected with autosomal dominant craniosynostosis. Cell. 1993; 75(3):443–50. [PubMed: 8106171]
10. Warren SM, Brunet LJ, Harland RM, Economides AN, Longaker MT. The BMP antagonist noggin regulates cranial suture fusion. Nature. 2003; 422(6932):625–9. [PubMed: 12687003]
11. Jiang X, Iseki S, Maxson RE, Sucov HM, Morriss-Kay GM. Tissue origins and interactions in the mammalian skull vault. Dev Biol. 2002; 241(1):106–16. [PubMed: 11784098]
12. Noden DM, Trainor PA. Relations and interactions between cranial mesoderm and neural crest populations. J Anat. 2005; 207(5):575–601. [PubMed: 16313393]

13. Yu HM, Jerchow B, Sheu TJ, Liu B, Costantini F, Puzas JE, Birchmeier W, Hsu W. The role of Axin2 in calvarial morphogenesis and craniosynostosis. Development. 2005; 132(8):1995–2005. [PubMed: 15790973]

14. Wang Y, Xiao R, Yang F, Karim BO, Iacovelli AJ, Cai J, Lerner CP, Richtsmeier JT, Leszl JM, Hill CA, Yu K, Ornitz DM, Elisseeff J, Huso DL, Jabs EW. Abnormalities in cartilage and bone development in the Apert syndrome FGFR2(+/S252W) mouse. Development. 2005; 132(15): 3537–48. [PubMed: 15975938]

15. Eswarakumar VP, Horowitz MC, Locklin R, Morriss-Kay GM, Lonai P. A gain-of-function mutation of Fgfr2c demonstrates the roles of this receptor variant in osteogenesis. Proc Natl Acad Sci U S A. 2004; 101(34):12555–60. [PubMed: 15316116]

16. Eswarakumar VP, Ozcan F, Lew ED, Bae JH, Tome F, Booth CJ, Adams DJ, Lax I, Schlessinger J. Attenuation of signaling pathways stimulated by pathologically activated FGF-receptor 2 mutants prevents craniosynostosis. Proc Natl Acad Sci U S A. 2006; 103(49):18603–8. [PubMed: 17132737]

17. Shukla V, Coumoul X, Wang RH, Kim HS, Deng CX. RNA interference and inhibition of MEK-ERK signaling prevent abnormal skeletal phenotypes in a mouse model of craniosynostosis. Nat Genet. 2007; 39(9):1145–50. [PubMed: 17694057]

18. Fukuda T, Scott G, Komatsu Y, Araya R, Kawano M, Ray MK, Yamada M, Mishina Y. Generation of a mouse with conditionally activated signaling through the BMP receptor, ALK2. Genesis. 2006; 44(4):159–67. [PubMed: 16604518]

19. Fukuda T, Mishina Y, Walker MP, DiAugustine RP. Conditional transgenic system for mouse aurora a kinase: degradation by the ubiquitin proteasome pathway controls the level of the transgenic protein. Mol Cell Biol. 2005; 25(12):5270–81. [PubMed: 15923640]

20. Bouxsein ML, Boyd SK, Christiansen BA, Guldberg RE, Jepsen KJ, Muller R. Guidelines for assessment of bone microstructure in rodents using micro-computed tomography. J Bone Miner Res. 2010; 25(7):1468–86. [PubMed: 20533309]

21. Mansukhani A, Bellosta P, Sahni M, Basilico C. Signaling by fibroblast growth factors (FGF) and fibroblast growth factor receptor 2 (FGFR2)-activating mutations blocks mineralization and induces apoptosis in osteoblasts. J Cell Biol. 2000; 149(6):1297–308. [PubMed: 10851026]

22. Yu PB, Deng DY, Lai CS, Hong CC, Cuny GD, Bouxsein ML, Hong DW, McManus PM, Katagiri T, Sachidanandan C, Kamiya N, Fukuda T, Mishina Y, Peterson RT, Bloch KD. BMP type I receptor inhibition reduces heterotopic [corrected] ossification. Nat Med. 2008; 14(12):1363–9. [PubMed: 19029982]

23. Wieser R, Wrana JL, Massague J. GS domain mutations that constitutively activate T beta R-I, the downstream signaling component in the TGF-beta receptor complex. EMBO J. 1995; 14(10): 2199–208. [PubMed: 7774578]

24. Yamauchi Y, Abe K, Mantani A, Hitoshi Y, Suzuki M, Osuzu F, Kuratani S, Yamamura K. A novel transgenic technique that allows specific marking of the neural crest cell lineage in mice. Dev Biol. 1999; 212(1):191–203. [PubMed: 10419695]

25. Soriano P. Generalized lacZ expression with the ROSA26 Cre reporter strain. Nat Genet. 1999; 21(1):70–1. [PubMed: 9916792]

26. Chen L, Li D, Li C, Engel A, Deng CX. A Ser252Trp [corrected] substitution in mouse fibroblast growth factor receptor 2 (Fgfr2) results in craniosynostosis. Bone. 2003; 33(2):169–78. [PubMed: 14499350]

27. Rice DP, Kim HJ, Thesleff I. Apoptosis in murine calvarial bone and suture development. Eur J Oral Sci. 1999; 107(4):265–75. [PubMed: 10467942]

28. Miraoui H, Marie PJ. Pivotal role of Twist in skeletal biology and pathology. Gene. 2010; 468(1-2):1–7. [PubMed: 20696219]

29. Yousfi M, Lasmoles F, El Ghouzzi V, Marie PJ. Twist haploinsufficiency in Saethre-Chotzen syndrome induces calvarial osteoblast apoptosis due to increased TNFalpha expression and caspase-2 activation. Hum Mol Genet. 2002; 11(4):359–69. [PubMed: 11854168]

30. Lemonnier J, Hay E, Delannoy P, Fromigue O, Lomri A, Modrowski D, Marie PJ. Increased osteoblast apoptosis in apert craniosynostosis: role of protein kinase C and interleukin-1. Am J Pathol. 2001; 158(5):1833–42. [PubMed: 11337381]

31. Kamiya N, Ye L, Kobayashi T, Mochida Y, Yamauchi M, Kronenberg HM, Feng JQ, Mishina Y. BMP signaling negatively regulates bone mass through sclerostin by inhibiting the canonical Wnt pathway. Development. 2008; 135(22):3801–11. [PubMed: 18927151]
32. Iseki S, Wilkie AO, Heath JK, Ishimaru T, Eto K, Morriss-Kay GM. Fgfr2 and osteopontin domains in the developing skull vault are mutually exclusive and can be altered by locally applied FGF2. Development. 1997; 124(17):3375–84. [PubMed: 9310332]
33. Iseki S, Wilkie AO, Morriss-Kay GM. Fgfr1 and Fgfr2 have distinct differentiation- and proliferation-related roles in the developing mouse skull vault. Development. 1999; 126(24):5611–20. [PubMed: 10572038]
34. Greenwald JA, Mehrara BJ, Spector JA, Warren SM, Fagenholz PJ, Smith LE, Bouletreau PJ, Crisera FE, Ueno H, Longaker MT. In vivo modulation of FGF biological activity alters cranial suture fate. Am J Pathol. 2001; 158(2):441–52. [PubMed: 11159182]
35. Holmes G, Rothschild G, Roy UB, Deng CX, Mansukhani A, Basilico C. Early onset of craniosynostosis in an Apert mouse model reveals critical features of this pathology. Dev Biol. 2009; 328(2):273–84. [PubMed: 19389359]
36. Mishina Y, Suzuki A, Ueno N, Behringer RR. Bmpr encodes a type I bone morphogenetic protein receptor that is essential for gastrulation during mouse embryogenesis. Genes Dev. 1995; 9(24): 3027–37. [PubMed: 8543149]
37. Zhang YE. Non-Smad pathways in TGF-beta signaling. Cell Res. 2009; 19(1):128–39. [PubMed: 19114990]
38. Ninomiya-Tsuji J, Kishimoto K, Hiyama A, Inoue J, Cao Z, Matsumoto K. The kinase TAK1 can activate the NIK-I kappaB as well as the MAP kinase cascade in the IL-1 signalling pathway. Nature. 1999; 398(6724):252–6. [PubMed: 10094049]
39. Steinbicker AU, Sachidanandan C, Vonner AJ, Yusuf RZ, Deng DY, Lai CS, Rauwerdink KM, Winn JC, Saez B, Cook CM, Szekely BA, Roy CN, Seehra JS, Cuny GD, Scadden DT, Peterson RT, Bloch KD, Yu PB. Inhibition of bone morphogenetic protein signaling attenuates anemia associated with inflammation. Blood. 2011; 117(18):4915–23. [PubMed: 21393479]
40. Boergermann JH, Kopf J, Yu PB, Knaus P. Dorsomorphin and LDN-193189 inhibit BMP-mediated Smad, p38 and Akt signalling in C2C12 cells. Int J Biochem Cell Biol. 2011; 42(11): 1802–7. [PubMed: 20691279]
41. Marie PJ, Debiais F, Hay E. Regulation of human cranial osteoblast phenotype by FGF-2, FGFR-2 and BMP-2 signaling. Histol Histopathol. 2002; 17(3):877–85. [PubMed: 12168799]
42. Ornitz DM, Marie PJ. FGF signaling pathways in endochondral and intramembranous bone development and human genetic disease. Genes Dev. 2002; 16(12):1446–65. [PubMed: 12080084]
43. Saito H, Kouhara H, Kasayama S, Kishimoto T, Sato B. Characterization of the promoter region of the murine fibroblast growth factor receptor 1 gene. Biochem Biophys Res Commun. 1992; 183(2):688–93. [PubMed: 1312839]
44. McEwen DG, Ornitz DM. Regulation of the fibroblast growth factor receptor 3 promoter and intron I enhancer by Sp1 family transcription factors. J Biol Chem. 1998; 273(9):5349–57. [PubMed: 9478995]
45. Hiyama A, Gogate SS, Gajghate S, Mochida J, Shapiro IM, Risbud MV. BMP-2 and TGF-beta stimulate expression of beta1,3-glucuronosyl transferase 1 (GlcAT-1) in nucleus pulposus cells through AP1, TonEBP, and Sp1: role of MAPKs. J Bone Miner Res. 2010; 25(5):1179–90. [PubMed: 19961337]
46. Fukuda T, Kohda M, Kanomata K, Nojima J, Nakamura A, Kamizono J, Noguchi Y, Iwakiri K, Kondo T, Kurose J, Endo K, Awakura T, Fukushi J, Nakashima Y, Chiyonobu T, Kawara A, Nishida Y, Wada I, Akita M, Komori T, Nakayama K, Nanba A, Maruki Y, Yoda T, Tomoda H, Yu PB, Shore EM, Kaplan FS, Miyazono K, Matsuoka M, Ikebuchi K, Ohtake A, Oda H, Jimi E, Owan I, Okazaki Y, Katagiri T. Constitutively activated ALK2 and increased SMAD1/5 cooperatively induce bone morphogenetic protein signaling in fibrodysplasia ossificans progressiva. J Biol Chem. 2009; 284(11):7149–56. [PubMed: 18684712]
47. Hu Q, Ueno N, Behringer RR. Restriction of BMP4 activity domains in the developing neural tube of the mouse embryo. EMBO Rep. 2004; 5(7):734–9. [PubMed: 15218525]

48. Shore EM, Xu M, Feldman GJ, Fenstermacher DA, Cho TJ, Choi IH, Connor JM, Delai P, Glaser DL, LeMerrer M, Morhart R, Rogers JG, Smith R, Triffitt JT, Urtizberea JA, Zasloff M, Brown MA, Kaplan FS. A recurrent mutation in the BMP type I receptor ACVR1 causes inherited and sporadic fibrodysplasia ossificans progressiva. Nat Genet. 2006; 38(5):525–7. [PubMed: 16642017]

49. van Dinther M, Visser N, de Gorter DJ, Doorn J, Goumans MJ, de Boer J, ten Dijke P. ALK2 R206H mutation linked to fibrodysplasia ossificans progressiva confers constitutive activity to the BMP type I receptor and sensitizes mesenchymal cells to BMP-induced osteoblast differentiation and bone formation. J Bone Miner Res. 2010; 25(6):1208–15. [PubMed: 19929436]

50. Rice DP, Aberg T, Chan Y, Tang Z, Kettunen PJ, Pakarinen L, Maxson RE, Thesleff I. Integration of FGF and TWIST in calvarial bone and suture development. Development. 2000; 127(9):1845–55. [PubMed: 10751173]

51. Rice R, Rice DP, Thesleff I. Foxc1 integrates Fgf and Bmp signalling independently of twist or noggin during calvarial bone development. Dev Dyn. 2005; 233(3):847–52. [PubMed: 15906377]

52. Wan DC, Pomerantz JH, Brunet LJ, Kim JB, Chou YF, Wu BM, Harland R, Blau HM, Longaker MT. Noggin suppression enhances in vitro osteogenesis and accelerates in vivo bone formation. J Biol Chem. 2007; 282(36):26450–9. [PubMed: 17609215]

53. Yamaguchi K, Nagai S, Ninomiya-Tsuji J, Nishita M, Tamai K, Irie K, Ueno N, Nishida E, Shibuya H, Matsumoto K. XIAP, a cellular member of the inhibitor of apoptosis protein family, links the receptors to TAB1-TAK1 in the BMP signaling pathway. EMBO J. 1999; 18(1):179–87. [PubMed: 9878061]

54. Lu M, Lin SC, Huang Y, Kang YJ, Rich R, Lo YC, Myszka D, Han J, Wu H. XIAP induces NF-kappaB activation via the BIR1/TAB1 interaction and BIR1 dimerization. Mol Cell. 2007; 26(5): 689–702. [PubMed: 17560374]

55. Perlyn CA, Morriss-Kay G, Darvann T, Tenenbaum M, Ornitz DM. A model for the pharmacological treatment of crouzon syndrome. Neurosurgery. 2006; 59(1):210–5. discussion 210-5. [PubMed: 16823318]

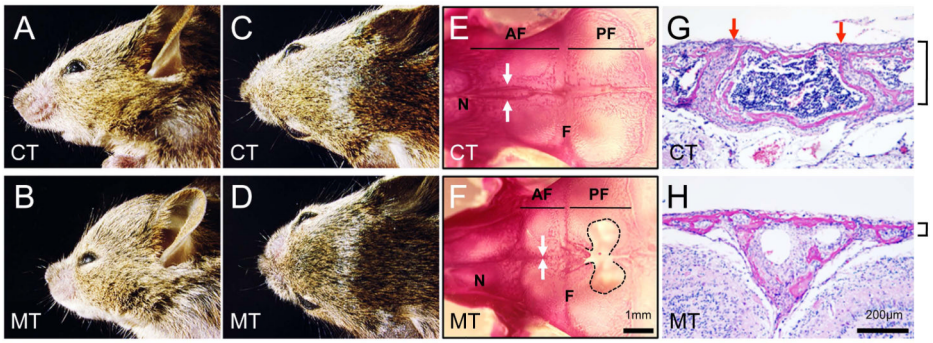

Fig. 1.

Enhanced BMP signaling through constitutively-active form of *Bmpr1a* causes craniosynostosis.

(A-D) *Ca-Bmpr1a:P0-Cre* (MT) displayed short broad snouts and hypertelorism at P17. (E, F) Skeletal staining at P17 revealed premature fusion in AF suture. AF suture was fused in *ca-Bmpr1a:P0-Cre* (F; white arrows), while AF suture in controls was still patent (E; white arrows). Along with premature fusion, foramina were developed in mutant's frontal bones (black dots). (G, H) H&E staining was performed on histological specimen at P8. AF suture in mutants displayed premature fusion (H) although AF suture in control showed patency (G; red arrows). The thickness of mutant skull was thinner than control (black lines). Abbreviations: AF, anterior frontal suture; F, frontal bone; N, nasal bone; PF, posterior frontal suture.

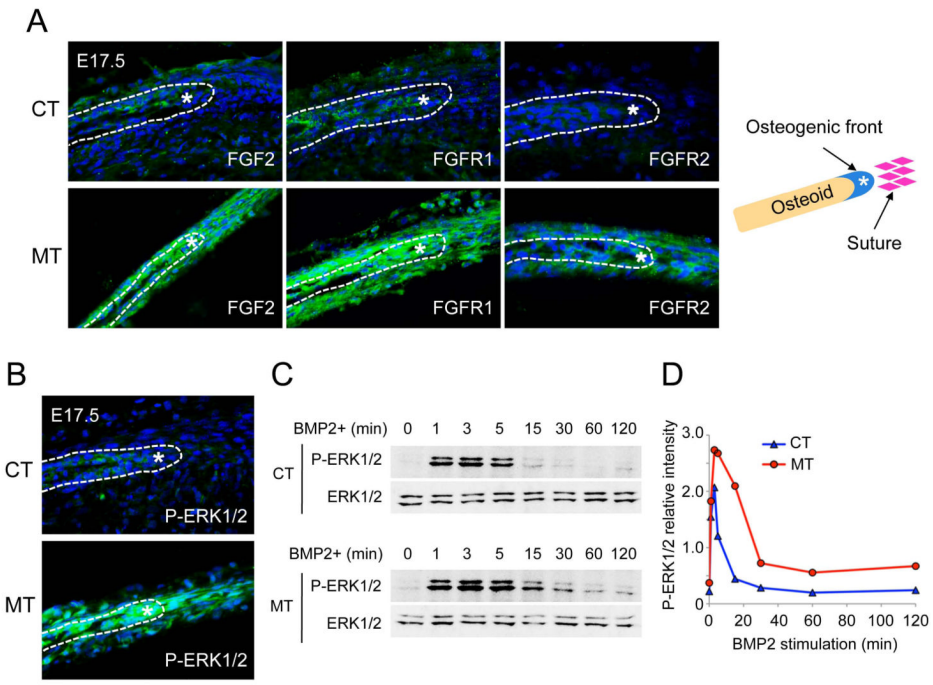

Fig. 2.

Enhancement of BMP signaling results in upregulation of FGF ligand, receptors and phospho-ERK1/2.

(A) Immunohistochemistry was performed by using FGF2, FGFR1 and FGFR2 antibodies (green) at E17.5. Levels of FGF2, FGFR1 and FGFR2 were upregulated in anterior frontal suture and osteoblasts in *ca-Bmpr1a:P0-Cre* (MT). (B) The levels of phospho-ERK1/2 (P-ERK1/2) in *ca-Bmpr1a:P0-Cre* at E17.5 were highly activated in comparison to controls (CT). Osteogenic front was marked by white asterisk. (C) Kinetics of ERK1/2 pathway activation following BMP2 stimulation. Preosteoblasts were stimulated with recombinant BMP2 (100 ng/ml) for the time indicated (min). Levels of P-ERK1/2 along with levels of total ERK1/2 proteins were measured by western blotting. Peak and sustained levels of P-ERK1/2 in *ca-Bmpr1a:P0-Cre* preosteoblasts were much higher than in control preosteoblasts. (D) Results in C for P-ERK1/2 quantified by densitometry.

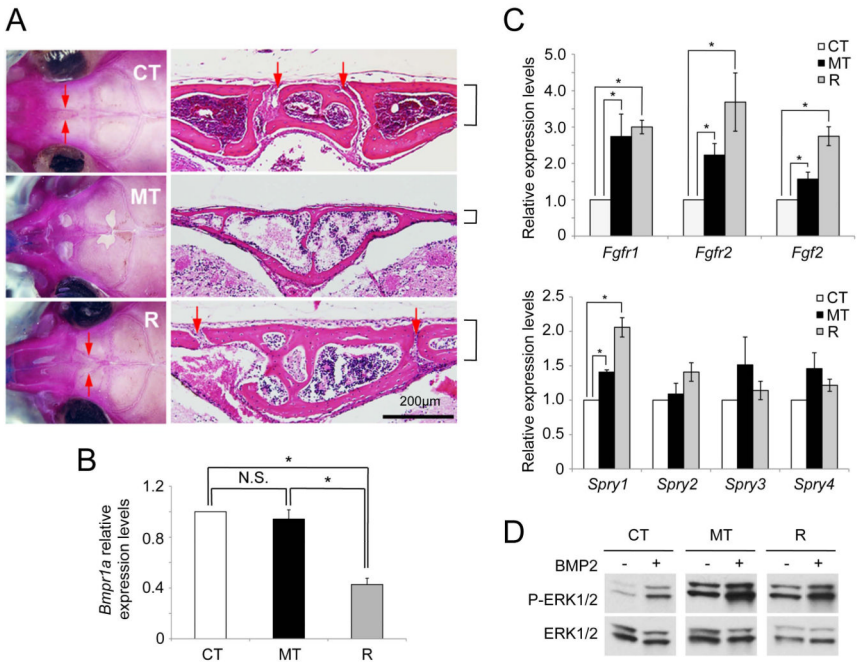

Fig. 3.

Heterozygous mutation of *Bmpr1a* rescues the phenotype of craniosynostosis.

(A) Heterozygous null mice for *Bmpr1a* also expressing a *P0-Cre* transgene were crossed with *ca-Bmpr1a*-transgenic mice. Heterozygosity of *Bmpr1a* rescued morphological abnormalities of craniofacial region developed in *ca-Bmpr1a:P0-Cre*. Skeletal staining was performed for skulls. Skull bone shapes were similar between both control (CT) and *ca-Bmpr1a:P0-Cre* carrying heterozygous null *Bmpr1a* (R). Patency of anterior frontal suture was confirmed by histological analysis. Red arrows indicated anterior frontal suture in control (CT) and *ca-Bmpr1a:P0-Cre* carrying heterozygous *Bmpr1a* (R). Note that bone thickness and foramen in frontal bone were also recovered in rescued skull (R) (black lines). (B) Expression of *Bmpr1a* was measured by quantitative real time RT-PCR (qRT-PCR) in preosteoblast cells from CNC-derived skull tissues. Open columns (control; CT), black columns (*ca-Bmpr1a:P0-Cre*; MT) and gray columns (*ca-Bmpr1a:P0-Cre* carrying heterozygous null *Bmpr1a*; R) were shown respectively. Data presented were means ± s.e.m. by three different preosteoblast cells from skull and three independent experiments. *p<0.05. (C) Expression of FGF ligand (*Fgf2*), receptors (*Fgfr1, Fgfr2*) and downstream targets (*Sprouty1, 2, 3, 4*) were measured by qRT-PCR in nasal and frontal bones at P4. Open columns (control; CT), black columns (*ca-Bmpr1a:P0-Cre*; MT) and gray columns (*ca-Bmpr1a:P0-Cre* carrying heterozygous null *Bmpr1a*; R) were shown respectively. Data presented were means ± s.e.m. by three different skulls and three independent experiments. *p<0.05. (D) Preosteoblasts from the skull were stimulated with recombinant BMP2 (100 ng/ml) and levels of phospho-ERK1/2 (P-ERK1/2) along with levels of total ERK1/2 proteins were measured by western blotting. The levels of P-ERK1/2 were still comparable between mutants (*ca-Bmpr1a:P0-Cre*) and rescued (*ca-Bmpr1a:P0-Cre* carrying heterozygous null *Bmpr1a*).

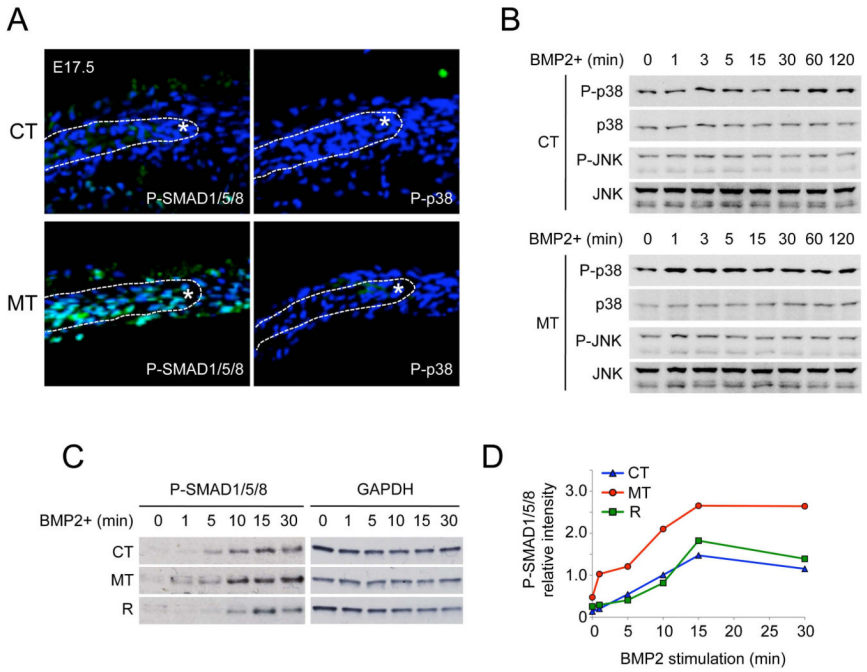

Fig. 4.

Enhanced Smad-dependent BMP signaling is responsible for developing craniosynostosis. (A) Immunohistochemistry using phospho-Smad1/5/8 (P-SMAD1/5/8) and phospho-p38 (P-p38) antibodies (green) were performed for calvarial sections at E17.5. Samples were counterstained with DAPI (blue). Osteogenic front is marked by white asterisk. (B) Kinetics of MAPK pathways activation following BMP2 stimulation in preosteoblasts of control (CT) and mutant (*ca-Bmpr1a:P0-Cre*; MT). Preosteoblasts were stimulated with recombinant BMP2 (100 ng/ml) for the time indicated (min). Levels of phospho-P38 (p-P38) and phospho-JNK (p-JNK) along with levels of total MAPK proteins were measured by western blotting. (C) Phospho-Smad1/5/8 (P-SMAD1/5/8) levels were examined in preosteoblasts of control (CT), mutant (*ca-Bmpr1a:P0-Cre*; MT) and rescued (*ca-Bmpr1a:P0-Cre* carrying heterozygous null *Bmpr1a*; R). Preosteoblasts were stimulated by recombinant BMP2 (100ng/ml) for indicated time (min) then P-SMAD1/5/8 levels were examined by western blotting. GAPDH was used as a loading control (upper panel). (D) Results for P-SMAD1/5/8 from *C* were quantified by densitometry (lower panel).

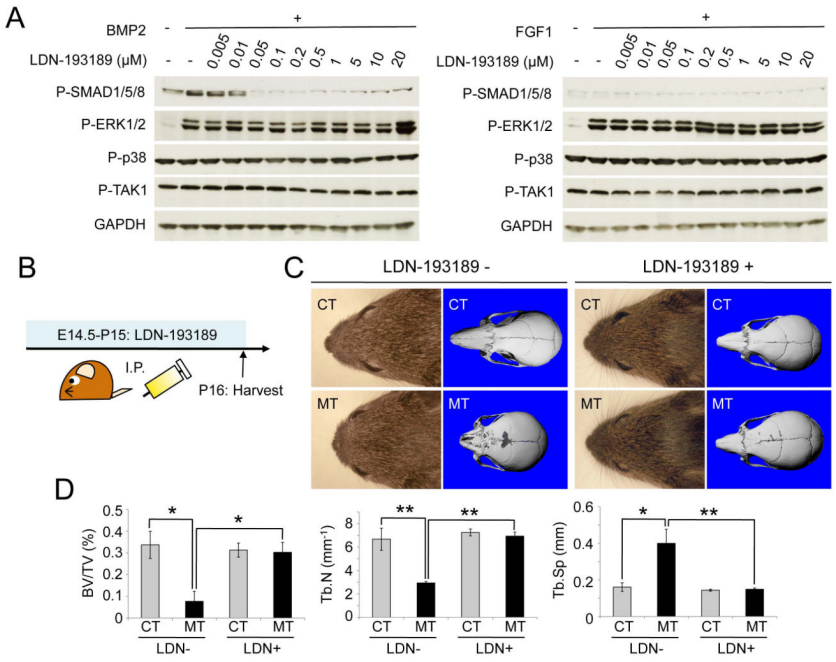

Fig. 5.

BMP type I receptor-specific chemical inhibitor LDN-193189 partially recovers the craniosynostosis phenotype in vivo.

(A) Wild-type preosteoblasts from skull were pretreated with LDN-193189 (0.005μM-20μM) for 30min. Subsequently preosteoblasts were stimulated by either BMP2 or FGF1 recombinant (100ng/ml) for 10min. Levels of phospho-Smad1/5/8 (P-SMAD1/5/8), phospho-ERK1/2 (P-ERK1/2), phospho-p38 (P-p38), phospho-TAK1 (P-TAK1) were examined by western blotting. GAPDH was used as a loading control. (B) Schematic representation of the dosing and harvesting schedule of LDN-193189 in vivo. (C) Lateral and top of view of face in control (CT) and *ca-Bmpr1a:P0-Cre* (MT) treated with LDN-193189. Note that short broad snouts and hypertelorism in *ca-Bmpr1a:P0-Cre* were partially recovered, which was comparable as control mice. (D) Bone volume (BV/TV), trabecular number (Tb.N) and trabecular spaces (Tb.Sp) in nasal and frontal bones were quantified by μCT. Data presented were means ± s.d. by three different skulls and three independent experiments. *p<0.05, **p<0.005.

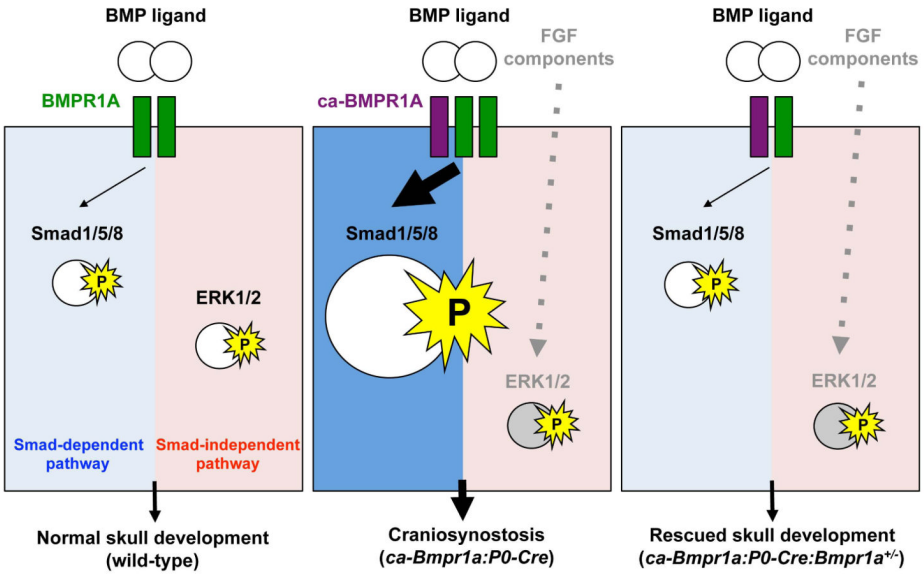

Fig. 6.

A mechanism by which enhanced BMP signaling develops craniosynostosis in mice. In wild–type skull, BMPR1A (green) exerts both Smad-dependent and - independent signaling upon ligand binding (left panel). In the mutant mice (*ca-Bmpr1a:P0-Cre*) which has a constitutively active form of BMPR1A (purple), basal levels of Smad-dependent signaling are upregulated and it is further increased upon ligand binding. Increases of phospho-ERK1/2 are also observed due to the increase of FGF signaling (middle panel). In the rescued mice (*ca-Bmpr1a:P0-Cre:Bmpr1a*$^{+/-}$), removal of one copy of endogenous BMPR1A normalizes levels of Smad-dependent signaling leading to the phenotypic rescue of premature suture fusions and skull morphology (right panel). Enhanced levels of FGF-ERK signaling are still observed in the rescued mice but it may be not sufficient to induce morphological malformations, i.e., FGF signaling in *ca-Bmpr1a:P0-Cre:Bmpr1a*$^{+/-}$ mice does not attain levels needed to develop craniosynostosis (see discussion),.